Inorganica Chimica Acta, 150 (1988) 65–73

A Convenient Synthetic Route to the Monocondensation Products of Pentane-2,4-dione and Aliphatic α,ω-Diamines. Synthesis, X-ray Structure and Magnetic Properties of a Trinuclear Copper(II) Complex with 8-Amino-5-aza-4-methyl-3-octene-2-one

MAREK KWIATKOWSKI*, EDMUND KWIATKOWSKI, ALEKSANDRA OLECHNOWICZ

Institute of Chemistry, University of Gdańsk, Sobieskiego 18, 80-952 Gdańsk, Poland

DOUGLAS M. HO and EDWARD DEUTSCH

Biomedical Chemistry Research Center and Department of Chemistry, University of Cincinnati, Cincinnati, Ohio 45221-0172, U.S.A.

(Received March 10, 1988)

Abstract

A convenient synthesis of four, new, tridentate-N_2O ligands which are monocondensation products of pentane-2,4-dione and aliphatic α,ω-diamines is described, and the basic properties of these ligands are reported. The reaction of one of them, 8-amino-5-aza-4-methyl-3-octene-2-one, HL^1, with copper(II) perchlorate affords the trinuclear μ_3-hydroxo bridged complex $[(CuL^1)_3(OH)](ClO_4)_2$. The single-crystal X-ray structure, spectroscopic and magnetic properties of this complex are described. The trinuclear cation consists of three CuL^1 subunits bound by a triply-bridging hydroxy group and three bridges formed by carbonyl oxygen atoms of three ligand molecules. Two trinuclear cations are held together within the unit cell by hydrogen bonding to the perchlorate anions. Crystallographic data: triclinic space group $P\bar{1}$ (No. 2), $a = 11.720(1)$, $b = 12.283(2)$, $c = 14.252(2)$ Å; $\alpha = 71.78(1)°$, $\beta = 81.07(1)°$, $\gamma = 65.69(1)°$, final R and R_w factors are 0.0418 and 0.0536 respectively. Magnetic susceptibility data indicate a weak antiferromagnetic exchange within the trinuclear core with $J = -15$ cm^{-1}.

Introduction

Recently, we reported [1] the synthesis of the monocondensation product between pentane-2,4-dione and 1,2-diaminoethane, *i.e.* 7-amino-5-aza-4-methyl-3-heptene-2-one HL^0. This compound proved to be an excellent intermediate for the preparation of a number of unsymmetrical tetradentate Schiff base ligands [1–7] by simple condensation of its free primary amino group with a carbonyl or ethoxymethylene group of a variety of reagents. Moreover, HL^0 can itself act as a tridentate ligand to accommodate a variety of coordination geometries [8–14]. Preparation of HL^0 is not straightforward since aliphatic diamines display a strong tendency for both primary amino groups to react with β-diketones; this consequently leads to symmetrical bis-imino tetradentate products [15]. In the preparation of HL^0 we utilized a several-fold excess of diamine (with respect to diketone) to prevent formation of the bis-imine product and favor condensation at only one end of the diamine. Further studies have revealed that this approach is generally applicable and in this paper we report the preparation of four new monocondensation products of pentane-2,4-dione and linear homologues of 1,2-diaminoethane. All of the resulting tridentate-N_2O ligands react readily with transition metal ions to form colored complexes. We report here the preparation, properties and single crystal X-ray structure of the Cu(II) complex isolated from the reaction of one of the monocondensation products, 8-amino-5-aza-4-methyl-3-octene-2-one, HL^1, with copper perchlorate. This compound, $[(CuL^1)_3(OH)](ClO_4)_2$, incorporates an interesting trinuclear Cu_3O_4 cluster formed by three copper atoms, three bridging carbonyl oxygen atoms, and one triply-bridging hydroxy group.

Experimental

Materials

Diamines (1,3-diaminopropane, 1,4-diaminobutane, 1,5-diaminopentane, 1,6-diaminohexane) and triethylamine were dried over potassium hydroxide and distilled prior to use. Pentane-2,4-dione was dried over anhydrous sodium sulphate and distilled; the fraction boiling at 138–139 °C was collected.

---

*On temporary leave from the University of Gdańsk. Author to whom correspondence should be addressed at the Department of Chemistry, University of Cincinnati, Cincinnati, Ohio 45221-0172, U.S.A.

0020-1693/88/$3.50

All other chemicals were reagent grade and were used without further purification.

Ligands HL^1–HL^4

Freshly distilled pentane-2,4-dione (0.05 mol) in 20 ml of absolute ethanol was added slowly to a vigorously stirred and cooled solution of the appropriate diamine (0.15 mol) in 120 ml of absolute ethanol. The temperature was maintained at *ca.* 10 °C. After the addition was complete, the mixture was stirred for an additional 15 min. Then the solvent and unreacted diamine were removed by evaporation and the oily residue was immediately distilled under reduced pressure. In this manner, the following ligands were obtained. HL^1: 8-amino-5-aza-4-methyl-3-octene-2-one, boiling point (b.p.) 110 °C/0.5 mmHg, yield 58%; HL^2: 9-amino-5-aza-4-methyl-3-nonene-2-one, b.p. 125 °C/0.2 mmHg, yield 53%; HL^3: 10-amino-5-aza-4-methyl-3-decene-2-one, b.p. 137 °C/0.2 mmHg, yield 47%; HL^4: 11-amino-5-aza-4-methyl-3-undecene-2-one, b.p. 140 °C/0.1 mmHg, yield 40%. The yields are relative to the amount of pentane-2,4-dione used.

(μ_3-Hydroxo)tris(μ-8-amino-5-aza-4-methyl-3-octene-2-onato)tricopper(II) Perchlorate, $[(CuL^1)_3(OH)](ClO_4)_2$

Copper perchlorate hexahydrate (0.01 mol) in methanol (50 ml) was refluxed with 2,2-dimethoxypropane for several hours in an attempt to obtain an anhydrous source of Cu(II). After evaporation of the solvents, the dark oily residue was redissolved in 50 ml of methanol and a solution containing 0.01 mol of HL^1 and 0.01 mol of anhydrous triethylamine was added. The mixture was stirred at room temperature for 1 h and then concentrated under reduced pressure to yield a precipitate of the copper complex. The complex was recovered by filtration, washed with cold methanol and recrystallized from methanol–diisopropyl ether to give $[(CuL^1)_3(OH)](ClO_4)_2$ as emerald green crystals. Melting point (m.p.) 187 °C; yield 50–60%. *Anal.* Found: C, 32.9; H, 5.3; N, 9.5. Calc. for $Cu_3C_{24}H_{46}N_6O_{12}Cl_2$: C, 33.0; H, 5.3; N, 9.6%.

Physical Measurements

Elemental analyses were performed on a Carlo Erba MOD 1106 Elemental Analyzer. FD (field desorption) mass spectra were recorded on a Varian MAT 711 spectrometer, ^{1}H NMR spectra on a Tesla BS487 80 MHz spectrometer, EPR spectra on a JES-ME-3X spectrometer working at 9 GHz, visible spectra on a Perkin-Elmer 402 spectrometer, and IR spectra on a Perkin-Elmer 621 spectrometer in Nujol or hexachlorobutadiene mulls. Conductance measurements were made with a K-58 conducting bridge constructed at the Technical University of Warsaw.

The magnetic susceptibility of the powdered copper complex was measured in the 4.5–290 K temperature range using a Faraday magnetometer. Mercury tetrakis(thiocyanato)cobaltate was used as the susceptibility standard, and the data were corrected for diamagnetism (estimated as -340×10^{-6} cgsu for the complex) and for TIP (the value of 60×10^{-6} cgsu per copper atom was used).

X-ray Crystallography of $[(CuL^1)_3(OH)](ClO_4)_2$

A suitable crystal of $[(CuL^1)_3(OH)](ClO_4)_2$ was isolated, mounted on the tip of a glass fiber with epoxy cement, and transferred to a Nicolet R3m four-circle diffractometer for characterization and data collection. Unit cell parameters were determined from the angular settings of 15 well-centered reflections ($20° < 2\theta < 29°$). Axial photographs, and a limited search through an octant of reciprocal space revealed a lack of systematic absences and symmetry indicating that the sample had crystallized in one of the triclinic space groups, *i.e.* $P1$ or $P\bar{1}$.

$\theta/2\theta$ scans were collected with variable scan speeds ranging from 2.0 to 29.3°/min. One hemisphere of data ($\pm h$, $\pm k$, $+l$) was collected with 2θ restricted to 3°–45°. A total of 4882 reflections were measured, and corrected for Lorentz-polarization and absorption effects (empirical absorption correction based on 5 azimuthal reflections). The minimum and maximum drift corrections were 0.9864 and 1.0051, respectively. Data averaging yielded 4307 unique reflections of which 3190 had $F > 6\sigma(F)$ with $R_{\text{int}} = 0.0149$.

The structure was successfully solved and refined by full-matrix least-squares in the triclinic space groups $P\bar{1}$ (No. 2). A combination of direct methods (SHELXS with the TREF option) and Fourier techniques were used to locate the positions of the non-hydrogen atoms. Isotropic refinement of this model with unit weights converged to $R = 0.0757$ with uncorrected data. Anisotropic refinement yielded $R = 0.0528$. Subsequent cycles of least-squares included absorption corrected data, a weighting scheme based on $\sigma(F)$, and hydrogen atoms riding on their respective carbon atoms with a C–H distance of 0.96 Å. The coordinates and isotropic temperature parameter for the hydroxy hydrogen atom H(4′) were free to vary. All of the N–H bond lengths were constrained to 0.87 Å with their respective H atom coordinates being free to vary. All of the C- and N-bound hydrogen atoms were assigned fixed isotropic parameters of 0.08 Å^2. The final values for the refinement indices are given in Table I along with the crystal data and data collection parameters. Fractional atomic coordinates and equivalent isotropic displacement parameters for the non-hydrogen atoms are assembled in Table II. See also ‘Supplementary Material’.

TABLE I. Structure Determination Summary for $[(CuL^1)_3(OH)](ClO_4)_2$

Crystal data	
Empirical formula	$C_{24}H_{46}Cl_2Cu_3N_6O_{12}$
Color and habit	emerald green prisms
Size (mm)	0.20 × 0.32 × 0.52
Space group	$P\bar{1}$ (No. 2)
Unit cell dimensions (Å)	a = 11.720(1) b = 12.283(2) c = 14.252(2)
Angles (°)	α = 71.78(1) β = 81.07(1) γ = 65.69(1)
Volume (Å^3)	1775.2(4)
Z (molecules/cell)	2
Molecular weight	872.20
Density, calc. (g/cm^3)	1.63
F(000) (e$^-$)	898
Data collection	
Diffractometer	Nicolet R3m
Radiation	Mo (0.71073)
Monochromator	highly oriented graphite crystal
Temperature	ambient (294 K)
hkl limits	± 14, ± 15, + 17
2θ range (°)	3–45
Scan type	$\theta/2\theta$
Scan speed (°/min)	variable, 2.0 to 29.3
Scan range (°)	0.8 below $K_{\alpha 1}$ to 0.8 above $K_{\alpha 2}$
Background measurement	stationary crystal and counter at beginning and end of scan; total background time to scan time ratio of 0.5
Standard reflections	3 measured every 37
Reflections collected	4882 total (4307 independent)
Reflections observed	3190; $F > 6\sigma(F)$
Absorption coefficient	19.61 cm^{-1}
No psi scan reflections	5
Min./max. transmission	0.713/0.901
Refinement	
System used	MicroVAX II; Nicolet SHELXS/ SHELXTL PLUS
Solution	direct methods (TREF)
Final residuals	R = 0.0418, R_w = 0.0536^a
Goodness-of-fit	S = 1.79^b
Largest |shift/e.s.d.|	0.001
Number of variables	438
Data-to-parameter ratio	7.3:1
Largest difference peak (e$^-$/Å^3)	0.76

[a] $R = \Sigma(|F_o| - |F_c|)/\Sigma(|F_o|)$, $R_w = [\Sigma(w||F_o| - |F_c||^2)/\Sigma(w|F_o|^2)]^{1/2}$, $w = [\sigma^2(F) + |g|F^2]^{-1}$, $g = 0.000427$. [b] $S = [\Sigma(w||F_o| - |F_c||^2)/(M - N)]^{1/2}$ where M is the number of observed reflections, and N is the number of parameters refined.

TABLE II. Fractional Atomic Coordinates (×10^4) and Equivalent Isotropic Displacement Parameters^a (Å^2 × 10^3) for $[(CuL^1)_3(OH)](ClO_4)_2$

Atom	x	y	z	U_{eq}
Cu(1)	7423.6(7)	3215.4(7)	7209.0(6)	34(1)
Cu(2)	9096.4(7)	3698.0(7)	8535.6(6)	32(1)
Cu(3)	7371.3(7)	6022.1(7)	6752.7(6)	33(1)
O(1)	7511(4)	2981(4)	8593(3)	43(2)
O(2)	7934(4)	5367(4)	8458(3)	38(2)
O(3)	6113(4)	5346(4)	6951(3)	40(2)
O(4)	8521(5)	4177(4)	7128(3)	32(2)
N(1)	7991(6)	3209(6)	5804(5)	50(3)
N(2)	6351(5)	2286(5)	7392(4)	38(3)
N(3)	10342(6)	2111(6)	8287(5)	55(3)
N(4)	9681(5)	3440(5)	9839(4)	40(3)
N(5)	8920(6)	6360(5)	6289(5)	42(3)
N(6)	6166(6)	7758(5)	6510(4)	44(3)
C(1)	7385(9)	2834(9)	5200(6)	65(5)
C(2)	6105(10)	3020(10)	5549(7)	82(6)
C(3)	5922(9)	2174(8)	6514(6)	67(5)
C(4)	5330(8)	878(8)	8356(6)	70(5)
C(5)	6050(6)	1690(6)	8267(6)	42(4)
C(6)	6344(7)	1745(6)	9162(5)	41(3)
C(7)	6998(6)	2347(6)	9314(5)	37(3)
C(8)	7164(8)	2361(7)	10333(5)	56(4)
C(9)	11334(9)	1232(8)	8989(7)	80(5)
C(10)	11743(9)	1866(10)	9482(9)	101(7)
C(11)	10858(8)	2399(8)	10245(7)	68(5)
C(12)	9418(8)	3830(7)	11475(5)	54(4)
C(13)	9030(7)	4124(7)	10432(5)	39(4)
C(14)	7927(7)	5205(7)	10139(5)	45(4)
C(15)	7462(6)	5787(6)	9218(5)	40(3)
C(16)	6341(8)	6987(8)	9015(7)	76(5)
C(17)	8943(8)	7607(6)	6086(6)	57(4)
C(18)	7780(9)	8599(7)	5606(7)	72(5)
C(19)	6621(8)	8798(7)	6188(7)	72(5)
C(20)	4080(8)	9372(7)	6699(7)	77(5)
C(21)	4950(7)	8057(6)	6722(5)	44(4)
C(22)	4390(6)	7172(7)	7033(5)	47(4)
C(23)	4936(6)	5942(7)	7131(5)	39(3)
C(24)	4176(7)	5147(8)	7474(7)	68(5)
Cl(1)	11977(2)	3660(2)	6189(1)	47(1)
O(5)	10825(5)	3717(5)	5907(4)	65(3)
O(6)	12678(6)	3987(7)	5342(5)	95(4)
O(7)	12663(6)	2439(6)	6718(6)	110(4)
O(8)	11684(6)	4468(8)	6768(7)	129(6)
Cl(2)	10132(2)	−106(2)	7086(2)	74(1)
O(9)	10342(7)	971(7)	6541(6)	113(2)
O(10)	9166(19)	−181(17)	6667(16)	129(7)
O(11)	9525(16)	226(15)	8000(13)	114(5)
O(12)	11149(16)	−1165(16)	7430(15)	112(5)
O(10′)	8949(16)	−248(15)	7235(14)	105(6)
O(11′)	10859(18)	−619(18)	7948(15)	130(6)
O(12′)	10895(16)	−1036(16)	6573(15)	129(6)

[a] Equivalent isotropic parameter U_{eq} defined as one third of the trace of the orthogonalized U_{ij} tensor.

Results and Discussion

Ligands

The formation of monocondensation products between pentane-2,4-dione and aliphatic α,ω-diamines was monitored by FD mass spectra of the reaction mixtures at various amine to diketone ratios. As previously observed for the pentane-2,4-

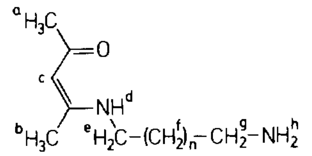

Fig. 1. Schematic representation of ligands; $n = 0$: HL^0, $n = 1$: HL^1, $n = 2$, HL^2, $n = 3$: HL^3, $n = 4$: HL^4; indexes a–h denote the protons for which NMR resonances are listed in Table III.

dione and 1,2-diaminoethane system [1], it has been found that at a three-fold excess of diamine, the monocondensation product was always the main species present in solution. In each case the monocondensation product can be readily isolated by vacuum distillation since it is fairly volatile and its boiling point differs markedly from those of the corresponding free amine and bis-imine. In this manner four new ligands HL^n ($n = 1$–4) have been obtained (Fig. 1). They are colorless, odorless, viscous liquids which decompose slowly at room temperature, although they can be stored for several days at −15 °C without any apparent signs of decomposition.

The pure ligands have been fully characterized by FD mass spectrometry and ^1H NMR spectrocopy (Table III). In the FD mass spectrum of each ligand a single peak corresponding to its molecular ion is observed. A key feature of the ^1H NMR spectrum of each of these ligands in chloroform is the presence of a quartet resonance at *ca.* 3.2 ppm, attributed to the methylene protons e (see Fig. 1). The quartet structure results from vicinal coupling with the neighboring CH_2 protons f plus additional coupling with the enamine proton d. This has been confirmed by the double resonance technique; irradiating the sample at the resonance frequency of proton d results in the collapse of the quartet structure into a simple triplet. These results indicate that all of the HL^n ligands reported here exist in their ketoenamine tautomeric form in chloroform solution.

Copper Complex [(CuL¹)₃(OH)](ClO₄)₂

Synthesis and Composition

The complex $[(CuL^1)_3(OH)](ClO_4)_2$ is prepared by the reaction of HL^1 with copper(II) perchlorate in methanol. Since the monocondensation products are rather sensitive to hydrolysis, the water of crystallization associated with copper perchlorate must be removed before the synthesis is conducted. This is accomplished by refluxing the salt dissolved in methanol with 2,2-dimethoxypropane. Anhydrous triethylamine is used as a non-coordinating base to consume the protons released from HL^1 during the synthesis.

Elemental analysis data are consistent with the formulation $[(CuL^1)_3(OH)](ClO_4)_2$ and the molar conductivity of the compound ($\lambda_M = 198\ \Omega^{-1}\ cm^2\ mol^{-1}$ in 10^{-3} M methanol) is within the range of 160–220 $\Omega^{-1}\ cm^2\ mol^{-1}$ typically observed for 1:2 electrolytes in 10^{-3} M methanolic solution [16]. The hydroxide ligand is presumably derived from traces of water present in the reaction medium.

Crystal structure

The structure consists of a dipositive trinuclear complex cation $[(CuL^1)_3(OH)]^{2+}$ and two non-coordinated perchlorate anions. A perspective view of the cation with its associated atom numbering scheme is depicted in Fig. 2, while the final bond distances and angles are presented in Tables IV and V. The trinuclear cation is comprised of three CuL^1 subunits in which each copper(II) cation is coordinated to a deprotonated tridentate monoanionic ligand L^1. The subunits, roughly perpendicular to each other, are bound together by a single, triply-bridging hydroxy group which is coordinated to each of the three copper centers, and by three bridging carbonyl oxygen atoms, each of them from a different ligand molecule (Fig. 3).

The three copper(II) ions and the bridging hydroxy group form a flattened trigonal pyramid with the copper sites roughly defining an equilateral triangle (the three Cu–Cu distances are 3.253, 3.278

TABLE III. Mass Spectrometric[a] and Proton NMR[b] Data of Ligands

Compound[c]	Molecular peak (m/z)	Chemical shifts δ (ppm)						
		a, b	c	d	e	f	g	h
HL^1	156	1.84s	4.90s	10.95br	3.20q	1.56qn	2.65t	1.71s
HL^2	170	1.80s; 1.84s	4.83s	10.77br	3.14q	1.46mp	2.58t	1.19s
HL^3	184	1.80s; 1.85s	4.90s	10.96br	3.19q	1.30br	2.61t	1.24s
HL^4	198	1.84s; 1.89s	4.91s	11.00br	3.20q	1.34br	2.63t	1.22s

[a] Molecular peaks observed in 8 kV FD mass spectrum. [b] Solutions in $CDCl_3$ with HMDS as internal reference; meaning of a–h is the same as in Fig. 1; s: singlet, t: triplet, q: quartet, qn: quintet, mp: multiplet, br: broadened band. [c] Ligand abbreviations are defined in the text (Fig. 1).

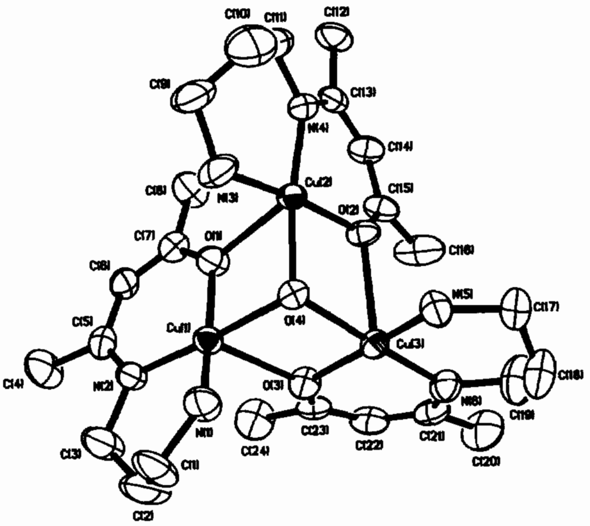

Fig. 2. A perspective view of the $[(CuL^1)_3(OH)]^{2+}$ cation including the atom numbering scheme. Hydrogen atoms are omitted for clarity.

and 3.317 Å, and the three Cu–Cu–Cu angles are 61.0°, 59.9° and 59.1°). The face-capping oxygen atom O(4) is situated approximately 0.77 Å above the Cu_3 plane. The Cu–O(4)–Cu angles are in the range 104.5°–108.4° which indicate sp^3 hybridization for the hydroxy oxygen atom. Each copper atom adopts a square pyramidal geometry, with the hydroxy oxygen atom and the three donor atoms of a single L^1 ligand occupying the four basal sites, and the carbonyl oxygen atom of a second L^1 moiety occupying the fifth apical position. Each carbonyl oxygen atom within the basal plane of one CuL^1 subunit is in turn apical to a copper atom in another subunit (Fig. 3).

There are only negligible discrepancies among the corresponding bond lengths and angles of the three CuL^1 subunits, however the overall structure lacks any element of three-fold symmetry. The Cu–O and Cu–N distances are not unusual and are comparable to those reported for analogous systems [9, 11]. The square pyramidal geometry within each subunit is distorted in the usual way, *i.e.* the copper ion is displaced from the basal plane towards the apical oxygen atom by 0.08–0.14 Å.

Two six-membered chelate rings are present in each subunit. The one incorporating the β-diketone core is essentially planar. A detailed examination of the bond lengths in this fragment of the molecule reveals that the C(5)–N(2) and C(6)–C(7) distances are relatively short (1.312 and 1.342 Å, respectively) and are close to typical double bond lengths (1.252–1.303 Å for C=N [17–19] and 1.337 Å for C=C [20]). On the other hand the C(5)–C(6) and C(7)–O(1) distances (1.399 and 1.311 Å, respectively) are relatively long for double bonds (typically 1.337

TABLE IV. Bond Distances (Å) for Non-hydrogen Atoms in $[(CuL^1)_3(OH)](ClO_4)_2$[a]

Cu(1)–O(1)	1.915(5)
Cu(1)–O(3)	2.368(4)
Cu(1)–O(4)	2.045(5)
Cu(1)–N(1)	2.011(6)
Cu(1)–N(2)	1.961(5)
Cu(2)–O(1)	2.343(4)
Cu(2)–O(2)	1.917(4)
Cu(2)–O(4)	2.044(5)
Cu(2)–N(3)	1.996(6)
Cu(2)–N(4)	1.967(5)
Cu(3)–O(2)	2.414(4)
Cu(3)–O(3)	1.918(4)
Cu(3)–O(4)	2.047(4)
Cu(3)–N(5)	1.995(6)
Cu(3)–N(6)	1.967(5)
O(4)–H(4′)	0.767(71)
O(1)–C(7)	1.311(8)
O(2)–C(15)	1.295(7)
O(3)–C(23)	1.296(7)
N(1)–C(1)	1.472(9)
N(2)–C(3)	1.483(9)
N(2)–C(5)	1.312(9)
N(3)–C(9)	1.472(10)
N(4)–C(11)	1.485(9)
N(4)–C(13)	1.310(8)
N(5)–C(17)	1.478(9)
N(6)–C(19)	1.499(9)
N(6)–C(21)	1.328(9)
C(1)–C(2)	1.451(12)
C(2)–C(3)	1.489(12)
C(4)–C(5)	1.519(9)
C(5)–C(6)	1.399(10)
C(6)–C(7)	1.342(9)
C(7)–C(8)	1.501(10)
C(9)–C(10)	1.443(12)
C(10)–C(11)	1.491(13)
C(12)–C(13)	1.511(9)
C(13)–C(14)	1.420(10)
C(14)–C(15)	1.358(9)
C(15)–C(16)	1.497(9)
C(17)–C(18)	1.487(10)
C(18)–C(19)	1.447(11)
C(20)–C(21)	1.507(9)
C(21)–C(22)	1.415(10)
C(22)–C(23)	1.347(9)
C(23)–C(24)	1.505(10)
Cl(1)–O(5)	1.437(5)
Cl(1)–O(6)	1.398(6)
Cl(1)–O(7)	1.397(6)
Cl(1)–O(8)	1.388(6)
Cl(2)–O(9)	1.406(8)
Cl(2)–O(10)	1.407(20)
Cl(2)–O(11)	1.475(17)
Cl(2)–O(12)	1.364(17)
Cl(2)–O(10′)	1.444(17)
Cl(2)–O(11′)	1.425(19)
Cl(2)–O(12′)	1.455(18)

[a] O(4)–H(4′) bond length is also included in this Table.

TABLE V. Bond Angles (°) for [(CuL^1)$_3$(OH)](ClO$_4$)$_2$

O(3)–Cu(1)–O(1)	92.2(2)
O(4)–Cu(1)–O(1)	81.3(2)
O(4)–Cu(1)–O(3)	71.7(2)
N(1)–Cu(1)–O(1)	159.7(2)
N(1)–Cu(1)–O(3)	99.5(2)
N(1)–Cu(1)–O(4)	86.6(2)
N(2)–Cu(1)–O(1)	94.5(2)
N(2)–Cu(1)–O(3)	107.9(2)
N(2)–Cu(1)–O(4)	175.7(2)
N(2)–Cu(1)–N(1)	97.7(2)
O(2)–Cu(2)–O(1)	93.3(2)
O(4)–Cu(2)–O(1)	71.7(2)
O(4)–Cu(2)–O(2)	81.5(2)
N(3)–Cu(2)–O(1)	88.7(2)
N(3)–Cu(2)–O(2)	167.1(2)
N(3)–Cu(2)–O(4)	87.0(2)
N(4)–Cu(2)–O(1)	114.3(2)
N(4)–Cu(2)–O(2)	93.6(2)
N(4)–Cu(2)–O(4)	172.6(2)
N(4)–Cu(2)–N(3)	97.2(3)
O(3)–Cu(3)–O(2)	97.3(2)
O(4)–Cu(3)–O(2)	70.4(2)
O(4)–Cu(3)–O(3)	81.8(2)
N(5)–Cu(3)–O(2)	91.6(2)
N(5)–Cu(3)–O(3)	162.2(2)
N(5)–Cu(3)–O(4)	86.7(2)
N(6)–Cu(3)–O(2)	105.9(2)
N(6)–Cu(3)–O(3)	94.6(2)
N(6)–Cu(3)–O(4)	174.3(2)
N(6)–Cu(3)–N(5)	97.9(2)
Cu(2)–O(1)–Cu(1)	99.1(2)
C(7)–O(1)–Cu(1)	126.4(4)
C(7)–O(1)–Cu(2)	132.9(4)
Cu(3)–O(2)–Cu(2)	99.3(2)
C(15)–O(2)–Cu(2)	124.1(4)
C(15)–O(2)–Cu(3)	134.7(4)
Cu(3)–O(3)–Cu(1)	99.3(2)
C(23)–O(3)–Cu(1)	134.1(4)
C(23)–O(3)–Cu(3)	124.4(4)
Cu(2)–O(4)–Cu(1)	105.4(2)
Cu(3)–O(4)–Cu(1)	106.5(2)
Cu(3)–O(4)–Cu(2)	108.3(2)
C(1)–N(1)–Cu(1)	121.6(5)
C(3)–N(2)–Cu(1)	119.5(5)
C(5)–N(2)–Cu(1)	122.6(5)
C(5)–N(2)–C(3)	117.8(6)
C(9)–N(3)–Cu(2)	121.5(6)
C(11)–N(4)–Cu(2)	121.9(5)
C(13)–N(4)–Cu(2)	122.7(5)
C(13)–N(4)–C(11)	115.3(6)
C(17)–N(5)–Cu(3)	122.5(5)
C(19)–N(6)–Cu(3)	120.2(5)
C(21)–N(6)–Cu(3)	122.4(5)
C(21)–N(6)–C(19)	117.0(6)
C(2)–C(1)–N(1)	110.9(7)
C(3)–C(2)–C(1)	117.3(8)
C(2)–C(3)–N(2)	115.8(6)
C(4)–C(5)–N(2)	120.0(7)
C(6)–C(5)–N(2)	124.4(6)
C(6)–C(5)–C(4)	115.6(7)
C(7)–C(6)–C(5)	129.0(6)
C(6)–C(7)–O(1)	122.9(6)
C(8)–C(7)–O(1)	115.4(6)
C(8)–C(7)–C(6)	121.7(6)
C(10)–C(9)–N(3)	111.7(7)
C(11)–C(10)–C(9)	116.2(9)
C(10)–C(11)–N(4)	113.9(7)
C(12)–C(13)–N(4)	122.2(7)
C(14)–C(13)–N(4)	122.7(6)
C(14)–C(13)–C(12)	115.1(6)
C(15)–C(14)–C(13)	127.9(6)
C(14)–C(15)–O(2)	123.8(6)
C(16)–C(15)–O(2)	114.9(6)
C(16)–C(15)–C(14)	121.3(6)
C(18)–C(17)–N(5)	111.4(6)
C(19)–C(18)–C(17)	117.6(8)
C(18)–C(19)–N(6)	117.2(6)
C(20)–C(21)–N(6)	121.4(7)
C(22)–C(21)–N(6)	123.2(6)
C(22)–C(21)–C(20)	115.4(7)
C(23)–C(22)–C(21)	128.2(7)
C(22)–C(23)–O(3)	124.8(6)
C(24)–C(23)–O(3)	114.8(6)
C(24)–C(23)–C(22)	120.4(6)
O(6)–Cl(1)–O(5)	109.5(4)
O(7)–Cl(1)–O(5)	108.6(4)
O(7)–Cl(1)–O(6)	108.5(5)
O(8)–Cl(1)–O(5)	108.0(4)
O(8)–Cl(1)–O(6)	111.3(5)
O(8)–Cl(1)–O(7)	110.9(6)
O(10)–Cl(2)–O(9)	110.0(9)
O(11)–Cl(2)–O(9)	101.7(7)
O(11)–Cl(2)–O(10)	102.5(11)
O(12)–Cl(2)–O(9)	118.0(8)
O(12)–Cl(2)–O(10)	118.9(11)
O(12)–Cl(2)–O(11)	102.6(10)
O(10′)–Cl(2)–O(9)	126.4(8)
O(11′)–Cl(2)–O(9)	106.6(8)
O(11′)–Cl(2)–O(10′)	114.6(11)
O(12′)–Cl(2)–O(9)	104.5(8)
O(12′)–Cl(2)–O(10′)	102.6(10)
O(12′)–Cl(2)–O(11′)	97.5(10)

Å for C=C and 1.23 Å for C=O [20]), but fall within the range observed for single bonds in conjugated systems. Thus, the bond lengths indicate that the coordinated L^1 ligand assumes an imino-enolic structure, in contrast to the ketoenamine structure of the non-coordinated HL^1 molecule (established by its ^{1}H NMR spectrum; *vide supra*).

The second six-membered chelate ring within each subunit incorporates the trimethylene fragment from the starting diamine, and assumes a half-boat conformation. Only minor variations are observed in the corresponding bond distances and angles within this ring and those of the other subunits. This is in contrast to what was reported for a similar copper complex with HL^0 [11] wherein a considerable

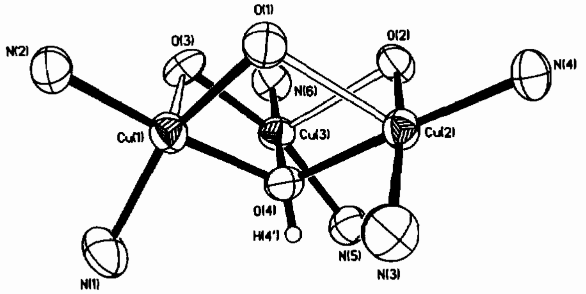

Fig. 3. An illustration of the Cu_3O_4 core structure of the $[(CuL^1)_3(OH)](ClO_4)_2$ complex.

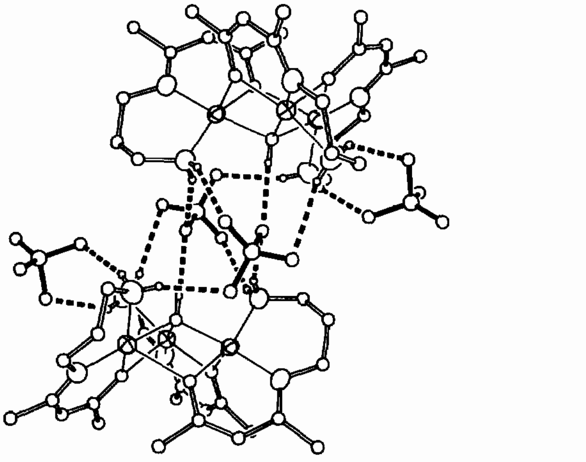

Fig. 4. An illustration of the hydrogen bonding interactions between the $[(CuL^1)_3(OH)]^{2+}$ cation and the perchlorate anions in the solid state.

degree of disorder was observed in the related five-membered chelate rings. Evidently, the more flexible six-membered rings in $[(CuL^1)_3(OH)](ClO_4)_2$ can better satisfy the coordination requirements of the copper ion than can the more highly strained five-membered rings of the HL^0 derivative.

Finally, additional aggregation is observed in the solid state due to the presence of hydrogen-bonding interactions between the $[(CuL^1)_3(OH)]^{2+}$ cations and the perchlorate anions. All six of the amine hydrogen atoms as well as the hydroxy H atom are involved in this hydrogen-bonding (with the two crystallographically independent perchlorate anions participating to different degrees). One of the two perchlorate anion sites exhibits rotational disorder, and is involved in only two peripheral hydrogen bonds. Aggregation is achieved solely through hydrogen-bonding with the other ordered perchlorate site. A view of the resulting dimeric centrosymmetric superstructure is presented in Fig. 4.

Properties

The IR spectrum of $[(CuL^1)_3(OH)](ClO_4)_2$ exhibits four absorption bands above 3000 cm^{-1} (3520, 3300, 3280, and 3165 cm^{-1}). The band at 3520 cm^{-1} appears within the range typical for O–H stretching vibrations in monohydroxo-bridged copper complexes [21] and is not present in the spectrum of the related $(CuL^1)_2Cl_2$ complex [22]. Therefore, this band is assigned to ν(OH) of the triply-bridging hydroxy group. The remaining bands arise from the N–H stretching vibrations. The presence of three such bands may be attributed to an unequal involvement of the two hydrogen atoms of the coordinated primary amino groups in hydrogen bonding. Hence, one of the two N–H vibrations, either the symmetric or antisymmetric, is split into two components. The presence of two differently situated perchlorate anions in the crystal structure supports this hypothesis. The absorption bands due to C=O, C=C, and C=N appear at 1595, 1570 and 1515 cm^{-1}, respectively. The perchlorate anions give rise to a broad feature at 1100 cm^{-1} (ν_3), a weak absorption band at 930 cm^{-1} (ν_1 forbidden in T_d symmetry) and a band at 625 cm^{-1} (ν_4). As the perchlorate anions are not coordinated to copper, the latter band shows no splitting [23].

In the visible spectrum of $[(CuL^1)_3(OH)](ClO_4)_2$ a single absorption band at 610 nm and a shoulder at approximately 420 nm are observed. The positions of these bands are consistent with the observed distorted square pyramidal geometry around the copper centers.

The magnetic susceptibility (and effective magnetic moment, μ_{eff}) of powdered samples of $[(Cu\text{-}L^1)_3(OH)](ClO_4)_2$ over 4.5–270 K are illustrated in Fig. 5. These plots indicate the presence of antiferromagnetic interactions within the trinuclear complex. As the temperature is lowered, μ_{eff} decreases from 1.80 at 290 K (μ_{eff} per trinuclear cation = 3.12)

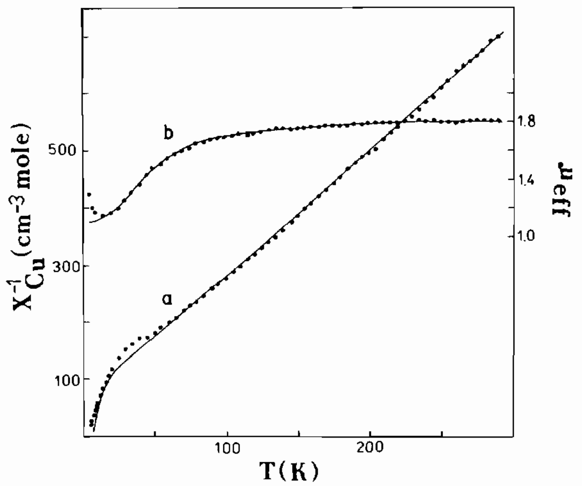

Fig. 5. Temperature dependence of the inverse magnetic susceptibilities χ_{Cu}^{-1} (a) and the magnetic moment μ_{eff} per copper atom (b) for $[(CuL^1)_3(OH)](ClO_4)_2$. The solid lines are theoretical fits based on eqn. (1) with $J = -15$ cm^{-1} and $g = 2.16$.

to 1.12 at 10 K (μ_{eff} per trinuclear cation = 1.94). When three paramagnetic metal ions of $S = 1/2$ are equivalent and form an equilateral triangle, the magnetic exchange interaction may be described by the single interchange parameter J. In the case of three copper(II) ions the corresponding equation has the following form [24]

$$\chi_M = \frac{Ng^2(\mu_B)^2}{4kT}\,\frac{1 + 5e^{3J/kT}}{1 + e^{3J/kT}} \qquad (1)$$

A least-squares fit of the data to this equation yields the values of $J = -15$ cm^{-1} and $g = 2.16$. The theoretical curves based on these optimized parameters and eqn. (1) are in reasonable agreement with the experimental data points as shown in Fig. 5.

The isotropic exchange interaction between three ions of $S = 1/2$ located at the apices of an equilateral triangle results in a splitting of the three degenerate energy levels into one quartet state with a total spin $S' = 3/2$, and two degenerate doublet states with $S' = 1/2$; the separation between the states is $-3J$, *i.e.* 45 cm^{-1} for $[(CuL^1)_3(OH)](ClO_4)_2$. The μ_{eff} value for the trinuclear unit at 10 K (1.94) indicates that at low temperatures the ground doublet states are predominantly occupied and the spin of the whole unit is close to 1/2. In the 10–100 K region, the excited quartet state becomes more and more accessible (its population increases with the temperature), and is almost entirely populated at 290 K. At the lowest temperatures (below 10 K), an increase of magnetic moment is observed. This is not expected for a trinuclear cluster and indicates weak ferromagnetic coupling between the trinuclear units.

The value of $J = -15$ cm^{-1} found for $[(CuL^1)_3(OH)](ClO_4)_2$ is considerably lower than the values reported for trinuclear hydroxo-bridged complexes with imine-oximato (-122 to -1000 cm^{-1}) [24] and pyrrazolato (-200 cm^{-1}) [25] ligands wherein the coordination planes of the three subunits are much more coplanar. On the other hand, the observed value corresponds well with the value of -12 cm^{-1} found for the more closely related $[(CuL^0)_3(OH)](ClO_4)_2$ derivative [11], wherein the coordination planes are roughly orthogonal. These observations imply that the degree of coplanarity of the three CuN_2O_2 coordination planes influences the magnetic coupling between the paramagnetic ions.

A powdered sample of $[(CuL^1)_3(OH)](ClO_4)_2$ shows no room-temperature EPR signal. At 77 K, a broad, weak signal is observed with a half-width value of *ca.* 680 gauss and a g value around 2.3. At 4.5 K, the spectrum consists of two main components observed at $g = 2.170$ and 1.970 with a shoulder at 2.045. The pattern presumably arises from the superposition of the doublet- and quartet-state spectra of the trinuclear unit, as well as from signals resulting from interactions among trinuclear units. The higher g value is close to the best-fit value of $g = 2.16$ obtained from the magnetic susceptibility data. Therefore, the broadened signal at $g = 2.170$ may be tentatively attributed to the doublet-state, and most likely represents the superposition of the parallel and perpendicular components.

Supplementary Material

Tables of anisotropic temperature parameters (Table VI), H atom coordinates and isotropic displacement parameters (Table VII), non-bonding and hydrogen-bonding interactions (distances and angles, Table VIII), least-squares planes (Table IX), and observed and calculated structure factors (Table X), as well as views of the CuL^1 subunits (Fig. 6), the two perchlorate anions (Fig. 7), and the trinuclear cation (Fig. 8, in stereo) are available upon request from author D.M.H.

Acknowledgements

This research was supported in part by Grant C.P.B.P.01.12 from the Polish Academy of Science and in part by Grant No. HL 21276 from the National Institutes of Health (E.D.). We are thankful to Prof. Jerzy Mroziński for his help in obtaining the magnetic susceptibility and EPR data.

References

1 E. Kwiatkowski and M. Kwiatkowski, *Inorg. Chim. Acta, 82,* 101 (1984).

2 E. Kwiatkowski, M. Kwiatkowski and A. Olechnowicz, *Inorg. Chim. Acta, 90,* 145 (1984).

3 E. Kwiatkowski and M. Kwiatkowski, *Inorg. Chim. Acta, 117,* 145 (1986).

4 J. P. Costes, G. Cros, M. H. Darbieu and J. P. Laurent, *Inorg. Chim. Acta, 60,* 111 (1982); *Transition Met. Chem., 7,* 219 (1982).

5 R. C. Coombes, J. P. Costes and D. E. Fenton, *Inorg. Chim. Acta, 77,* L173 (1983).

6 J. P. Costes, G. Cros and J. P. Laurent, *Inorg. Chim. Acta, 97,* 211 (1985).

7 H. Adams, N. A. Bailey, I. S. Bard, D. E. Fenton, J. P. Costes, G. Cros and J. P. Laurent, *Inorg. Chim. Acta, 101,* 7 (1985).

8 G. Cros and J. P. Costes, *C. R. Acad. Sci. Paris, 294-II,* 173 (1982).

9 J. P. Costes, F. Dahan and J. P. Laurent, *J. Coord. Chem., 13,* 355 (1984).

10 J. P. Costes, *Transition Met. Chem., 10,* 185 (1985).

11 J. P. Costes, F. Dahan and J. P. Laurent, *Inorg. Chem., 25,* 413 (1986).

12 J. P. Costes, J. F. Serra, F. Dahan and J. P. Laurent, *Inorg. Chem., 25,* 2790 (1986).

13 J. P. Costes, G. Commenges and J. P. Laurent, *Inorg. Chim. Acta, 134,* 237 (1987).

14 J. P. Costes and J. P. Laurent, *Inorg. Chim. Acta, 134,* 245 (1987).

15 A. E. Martell, R. L. Belford and M. Calvin, *J. Inorg. Nucl. Chem., 5,* 170 (1955).

16 W. J. Geary, *Coord. Chem. Rev.*, *7*, 81 (1971).
17 F. Akhtar and M. G. B. Drew, *Acta Crystallogr., Sect. B*, *38*, 1149 (1982).
18 W. Mazurek, K. J. Berry, K. S. Murray, M. J. O'Connor, M. R. Snow and A. G. Wedd, *Inorg. Chem.*, *21*, 3071 (1982).
19 F. Nepveu, J. P. Laurent and J. J. Bonnet, *Acta Crystallogr., Sect. C*, *39*, 339 (1983).
20 O. Kennard, in K. Lonsdale (ed.), 'International Tables for X-ray Crystallography', Vol. 3, Kynoch Press, Birmingham, 1962, Chap. 4.2, p. 276.
21 J. R. Ferraro and W. R. Walker, *Inorg. Chem.*, *4*, 1382 (1965).
22 M. Kwiatkowski, E. Kwiatkowski and A. Olechnowicz, work in progress.
23 K. Nakamoto, 'Infrared Spectra of Inorganic and Coordination Compounds', Wiley, New York, 1970, pp. 173, 175.
24 R. J. Butcher, C. J. O'Connor and E. Sinn, *Inorg. Chem.*, *20*, 537 (1981).
25 F. B. Huisbergen, R. W. M. Ten Hoedt, G. C. Verschoor and J. Reedijk, *J. Chem. Soc., Dalton Trans.*, 539 (1983).